Kinetic Behavior of the SAPO−18 Catalyst in the Transformation of Methanol into Olefins

ARTICLE *in* INDUSTRIAL & ENGINEERING CHEMISTRY RESEARCH · JULY 2005

Impact Factor: 2.59 · DOI: 10.1021/ie050110k

Kinetic Behavior of the SAPO-18 Catalyst in the Transformation of Methanol into Olefins

Ana G. Gayubo,* Raquel Vivanco, Ainhoa Alonso, Beatriz Valle, and Andrés T. Aguayo

Departamento de Ingeniería Química, Universidad del País Vasco, Apartado 644, 48080 Bilbao, Spain

Kinetic behavior (production of olefins, selectivity) has been studied in the transformation of methanol into olefins on a catalyst prepared based on SAPO-18 in a fluidized bed reactor, for a wide range of operating conditions (temperature, space time, concentration of methanol in the feed, dilution of methanol with water, time on stream). Under certain conditions, an initiation period is observed, which is in agreement with the "carbon pool mechanism" and whose duration largely depends on the operating conditions and, particularly, on water content in the reaction medium. A study has been carried out on the role of water as an inhibiting agent in the formation of olefins and in coke deposition. The methanol/dimethyl ether ratio is higher than that corresponding to thermodynamic equilibrium under conditions in which the catalyst is active for olefin formation. The hydrothermal stability of SAPO-18 has been proven by using the catalyst in a series of 10 successive cycles of reaction−regeneration.

Introduction

The interest in the methanol to olefins (MTO) process is justified by the increase in the demand for olefins, which are used as raw materials in the petrochemical industry and for the synthesis of fuels for diesel engines. The transformation of methanol and other oxygenates (such as bioethanol or biomass pyrolysis liquid) into olefins is an attractive route because of the rising trend in oil prices and also because of the availability without geographic limits of alternative resources to oil (natural gas, coal, biomass). Furthermore, considerable progress has been made in the technological development of the reactions required, first, for obtaining syngas and, subsequently, for methanol synthesis.[1,2] Among the different sources for syngas, re-forming of natural gas is more profitable than biomass gasification for methanol synthesis.[2] An additional incentive for methanol synthesis is the contribution to CO_2 balance by incorporating it as a raw material together with syngas.[3]

Ever since the initial proposal of the MTO process on the HZSM-5 zeolite and in order to fill the gap in the MTG process for obtaining automotion gas−oil, numerous studies have been carried out that are aimed at improving the catalyst in order to increase selectivity to light olefins. The aim of these studies is to reduce the number and strength of the acid sites or to increase shape selectivity. The modification of the acid structure of the HZSM-5 zeolite has been carried out: by increasing the Si/Al ratio;[4,5] by treatment with compounds that contain P and Mg;[6,7] by substitution of Si^{4+} by Fe^{3+};[8] by selectively poisoning the acid sites with organic bases;[9] by isomorphic substitution of Al^{3+} by trivalent cations[10] or by transition metals or V.[11]

Attempts have been made to increase the shape selectivity of the HZSM-5 zeolite by increasing the diffusional restrictions of its porous structure by depositing SiO_2 onto its structure[12] or by adding the zeolite to an amorphous matrix of SiO_2/Al_2O_3.[13] Most of the aforementioned modifications also increase the hydrothermal stability of the HZSM-5 zeolite. This property is essential in view of the severe conditions of high temperature and high content of water in the reaction medium in the MTO process.

Kaiser[14,15] was the first to study the behavior of silicoaluminophosphate (SAPO) molecular sieves on the conversion of methanol to light olefins. The structures of these materials are topologically similar to zeolites of small pore size: SAPO-34 (structure of CHA type), SAPO-17 (ERI), SAPO-35 (LEV), SAPO-44 (CHA), and SAPO-16 (AST). The one more studied is SAPO-34, whose deactivation by coke is very fast,[16,17] although activity is completely recovered after coke combustion with air.[18]

SAPO-18 (AEI structure) is isostructural to $AlPO_4$-18, and its structure is also related to chabazite/SAPO-34.[19] Chen et al.[20,21] proved that the initial catalytic activity for conversion of methanol on SAPO-18 is very similar to that on SAPO-34, whereas the life of the catalyst is much longer.[22,23] Furthermore, the latter researchers pointed out the lower preparation cost of SAPO-18, which is due to the simplicity of the preparation method and because the latter requires an organic template of lower cost than that corresponding to SAPO-34.

This paper aims to further the knowledge of the kinetic behavior of SAPO-18 in the MTO process and, accordingly, the effect of the operating conditions (temperature, space time, content of water in the feed, time on stream) on its activity, selectivity to olefins, product distribution, and recovery of activity in successive reaction−regeneration cycles is studied.

Experimental Section

The catalyst is made up of SAPO-18 as active phase (25 wt %), which is agglomerated by wet extrusion with bentonite (Exaloid) as binder (45 wt %) and with inert alumina (Prolabo) as charge (30 wt %). SAPO-18 has been synthesized following the method of Chen et al.[21] SAPO-18 crystals have an equivalent diameter of 4.13

* To whom correspondence should be addressed. Tel: 34-94-6015449. Fax: 34-94-6013500. E-mail: iqpgacaa@lg.ehu.es.

10.1021/ie050110k CCC: $30.25
Published on Web 07/12/2005

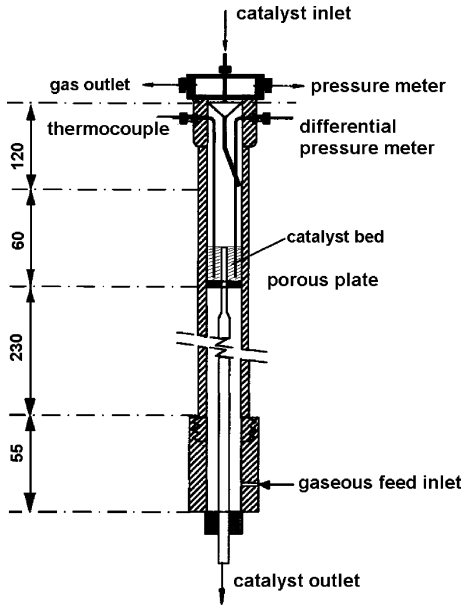

Figure 1. Scheme of the fluidized bed reactor.

μm (determined by laser ray difraction in a Malvern Mastersizer). Agglomeration first confers upon the catalyst a high mechanical resistance to attrition, which is required for its commercial use in a fluidized bed reactor. Furthermore, SAPO-18 particles with micropores of 3.8-Å diameter are embedded in a mesoporous structure (common to bentonite and alumina), which gives the reaction components improved access to the catalyst and better circulation, with enhanced heat dissipation, either in the reaction stage or in regeneration by coke combustion, given that both are highly exothermal. The last step in the preparation is the calcination of the catalyst at 575 °C for 2 h. The calcined catalyst is stored in hermetically sealed vessels in order to avoid water retention in the catalyst pores. The physical properties of the catalyst determined by N_2 adsorption−desorption and Hg porosimetry are as follows: BET surface area, 171 $m^2\ g^{-1}$; macropore volume, 0.15 $cm^3\ g^{-1}$; mesopore volume, 0.24 $cm^3\ g^{-1}$; micropore volume, 0.13 $cm^3\ g^{-1}$. The pore volume distribution is as follows: d_p < 20 Å, 25%; 20 Å < d_p < 500 Å, 46%; 500 Å < d_p, 29%.

From the thermogravimetric measurement of NH_3 adsorption, a total acidity of 0.12 (mmol of NH_3)(g of catalyst)$^{-1}$ has been determined at 150 °C. By combining thermogravimetric and calorimetric measurements, acid strength has been proven to be very uniform with a majority of sites with adsorption heat of 140−150 kJ (mol of NH_3)$^{-1}$ and with peaks in the TPD of NH_3 at 243 °C (weak acidity) and at 331 °C (strong acidity). Consequently, the sites are moderately acid and their density is lower than in the SAPO-34.[23]

The study of the effect of the operating conditions on the kinetic behavior of SAPO-18 has been carried out in reaction equipment provided with a fluidized bed reactor. The reactor (Figure 1) is a vertical cylinder of S-316 stainless steel of 20-mm internal diameter and a total length of 465 mm, which is located within a ceramic chamber heated by an electric resistance. It is provided with a porous plate for supporting the catalyst bed, which is placed at 285 mm from the bottom. Methanol (and water, as applicable) is fed by means of a high-precision digital plug pump (Gilson 307), with a flow rate range from 0.025 to 5 mL min^{-1}, to a chamber that works as a vaporizer−preheater, where it is mixed with the inert gaseous stream (N_2) coming from the line of gases. The gas flow rate is measured by means of a F-111C-HD-11-V mass flow meter (Bronkhorst High-Tech B.V.). The vaporized reactant mixture passes through a filter and enters the reactor through the lower part. The absolute pressure is controlled by a pressure meter.

The temperatures of the catalytic bed and of the vaporization chamber are measured by thermocouples and are regulated by digital controllers (whose thermocouples are introduced into the catalytic bed and into the oven, respectively).

The reaction products leave the reactor through the upper part by passing through two filters in series (the first one for particles of up to 20 μm and the second one of high efficiency, for particles of up to 2 μm) in order to avoid the passage of fine catalyst particles into the line of gases. Subsequently, they pass to a six-port valve operated by compressed air. When this valve is activated (manually or from the main computer), a sample of the product is retained in a loop and is sent to the device for gas analysis. This sample leaves the reaction equipment through a line thermostated at 170 °C, which is controlled by a digital temperature controller.

The reaction gases that do not pass through the analysis equipment are cooled to 0 °C in a partial condenser, and the products are collected in an intermediate vessel whose level is regulated by a level controller. Two streams leave this condenser; the first one consists of the uncondensable gases that leave the reaction equipment through an outlet and the second is the condensed liquid, which is collected in a vessel placed on an EK-600H digital balance (Electronic Balances) in order to monitor the nonreacted mass.

The catalytic bed is a captive fluidized bed. It consists of a mixture of the catalyst with a particle size between 150 and 250 μm and inert alumina with a particle size between 60 and 90 μm, with a catalyst/inert ratio of 20/80 in weight. Accordingly, the hydrodynamic properties of the bed are improved. The minimum fluidization velocity is 0.87 cm s^{-1} and corresponds to a gas flow rate of 163 $cm^3\ min^{-1}$. By means of runs with gaseous tracers, it has been determined that, in the range of conditions studied, gas flow deviation from plug flow is small.

The operating variables are controlled by means of Adkir process control software, which has been specifically designed for this process. Communication between all the digital controllers corresponding to the system variables and the computer is carried out through a E.I.A. Standard RS-485 communication line. The communication language between the computer and the peripheral hardware is ASCII.

The on-line analysis of the reaction products is carried out by means of a Varian Star 3400 CX gas chromatograph provided with a flame ionization detector. A capillary column (PONA cross-linked methyl silicone, 50 m × 0.2 mm × 0.5 μm) has been used with a flow rate for the carrier gas (He) of 1 $cm^3\ min^{-1}$. Communication between the reaction equipment and the chromatograph is carried out through a digital controller (RS-485 communication line with the central computer). The analysis conditions are as follows: initial temperature of the chromatograph oven, 35 °C; initial time at 35 °C, 2 min; temperature increase ramp, 20 °C min^{-1}; final temperature, 55 °C; time at 55 °C, 1 min; temper-

ature decrease ramp, 40 °C min^{-1}; final time at 35 °C, 0 min. The total duration of the analysis is 4.5 min.

In studies on reaction−regeneration and after the reaction stage, the catalytic bed is subjected to a sweeping treatment with N_2 for 30 min following a temperature ramp from the reaction temperature to 550 °C. The regeneration of the catalyst is carried out at this temperature by changing the N_2 stream for an air stream. The time of the regeneration stage is 2 h, which is long enough to completely eliminate the coke deposited in all the operating conditions.

Results

Effect of Operating Conditions on the Conversion of Methanol. Total conversion to hydrocarbons, X_T, has been determined as the sum of all the yields of individual hydrocarbon products, which are the mass fractions of each i component by mass unit of organic components in the product stream (hydrocarbons + oxygenates). The products that are obtained in significant amount are C_2-C_5 olefins and, above 425 °C, methane. The maximum yield of methane is 2% at 475 °C and is obtained in runs in which no water is fed with methanol. Figures 2-4 show the effect of temperature (Figure 2), space time (Figure 3), and water content in the feed (Figure 4) on the evolution of conversion with time on stream. Each figure contains three graphs corresponding to different operating conditions.

It is observed that conversion of oxygenates increases with temperature (Figure 2) and with space time (Figure 3) when the remaining conditions are the same. The increase in water content in the feed when the remaining conditions are the same (Figure 4), on one hand, gives way to a decrease in the conversion of oxygenates but, on the other hand, attenuates deactivation caused by coke deposition. This effect of water is well documented in the transformation of methanol into hydrocarbons on HZSM-5 zeolite[24,25] and on SAPO-34[16,17,26−28] and is a consequence of the adsorption of water on the acid sites competing with the adsorption of methanol and coke precursors. This second effect seems to be more important, although given the complexity of water effect, water in the feed is a key condition to be optimized in the MTO process at industrial scale. This optimization requires kinetic models for the MTO process and for coke deactivation, in which the effect of water in the reaction medium must be taken into account.

It is noteworthy that, under certain operating conditions (Figures 2b, c, 3b, c, and 4a, b), conversion is initially zero for the fresh catalyst, and subsequently, once a period of time has elapsed, it increases very quickly. This result agrees with the carbon pool mechanism, whose postulate is that the formation of reactive intermediates (methylarene-type compounds) trapped in the cages of SAPO-18 is required for the formation of olefins.[29−31] The presence of these intermediates is well proven by means of the spectroscopic analysis of different acid catalysts (SAPO-34, ZSM-5, β-zeolites).[32−34]

The results of conversion with time on stream allow for establishing that conversion evolves according to three successive periods: initiation, olefin production (which passes through a peak), and deactivation. According to the carbon pool mechanism, the existence of these three periods is explained by the evolution in the formation of active intermediates and their degradation to coke with time on stream. Thus, conversion decreases

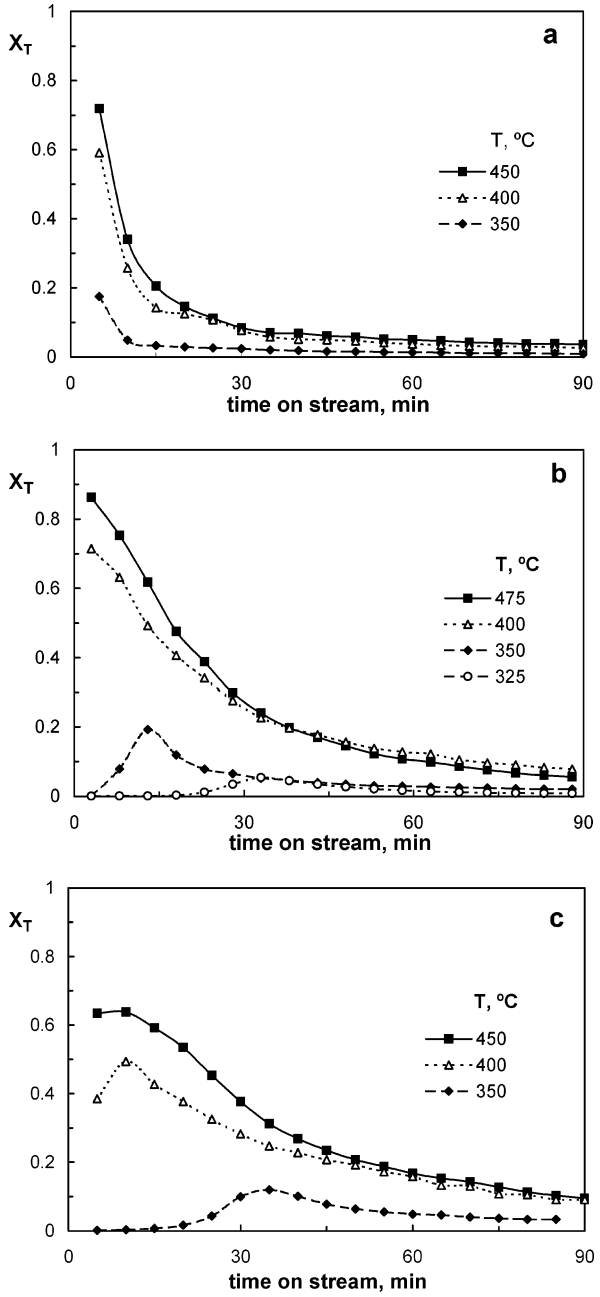

Figure 2. Evolution of conversion with time at different temperatures. (a) W/F_{M0} = 0.099 (g of catalyst)h(g of methanol)$^{-1}$ and X_{W0} = 0 (g of water)(g of methanol)$^{-1}$. (b) W/F_{M0} = 0.174 (g of catalyst)h(g of methanol)$^{-1}$ and X_{W0} = 1 (g of water)(g of methanol)$^{-1}$. (c) W/F_{M0} = 0.165 (g of catalyst)h(g of methanol)$^{-1}$ and X_{W0} = 3 (g of water) (g of methanol)$^{-1}$.

when degeneration of active intermediates is more rapid than their formation. Degeneration of intermediates consists of their dehydrogenation and condensation to form coke components, which are more easily developed in SAPO-18 cages and, consequently, block access of methanol to the pores. In a previous paper, deposition of these intermediates on SAPO-18 and their relationship with the initiation step prior to olefin formation has been studied by thermogravimetric monitoring.[35]

The initiation period has already been observed by Chen et al.[36] in the transformation of methanol into olefins on SAPO-34, although it was under conditions in which reaction rate was very limited and conversion was very low. Moreover, Guisnet studied other catalytic reactions in which reactive intermediates retained in

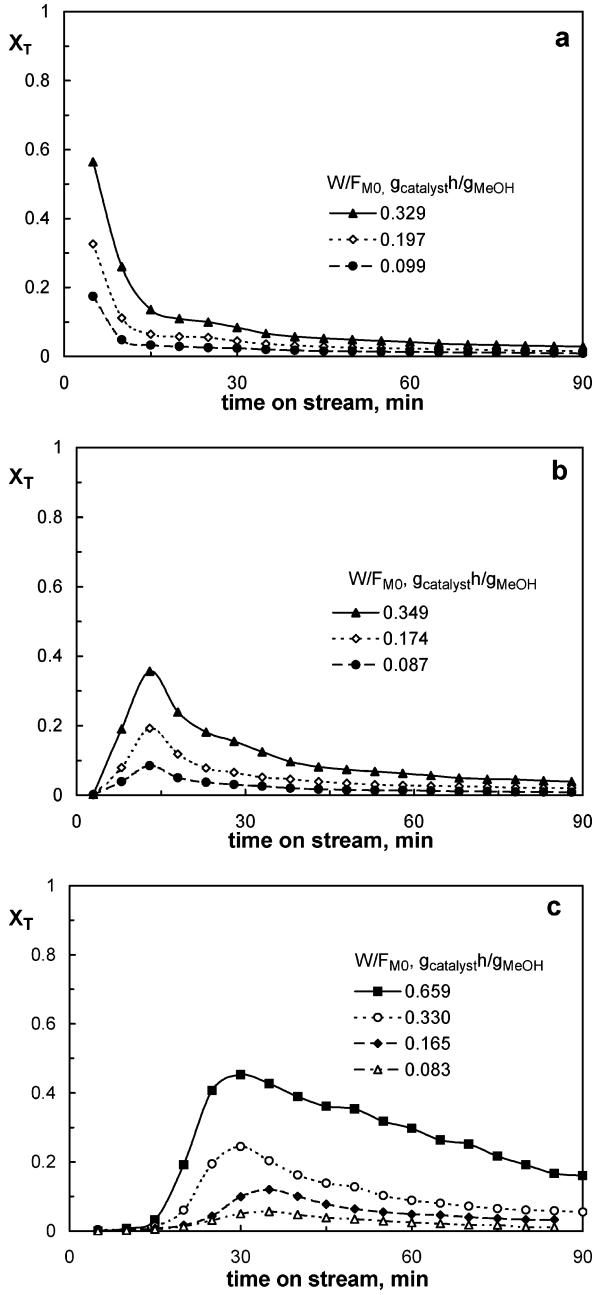

Figure 3. Evolution of conversion to hydrocarbons with time on stream at 350 °C for different values of space time. (a) $X_{W0} = 0$ (g of water)(g of methanol)$^{-1}$. (b) $X_{W0} = 1$ (g of water)(g of methanol)$^{-1}$. (c) $X_{W0} = 3$ (g of water)(g of methanol)$^{-1}$.

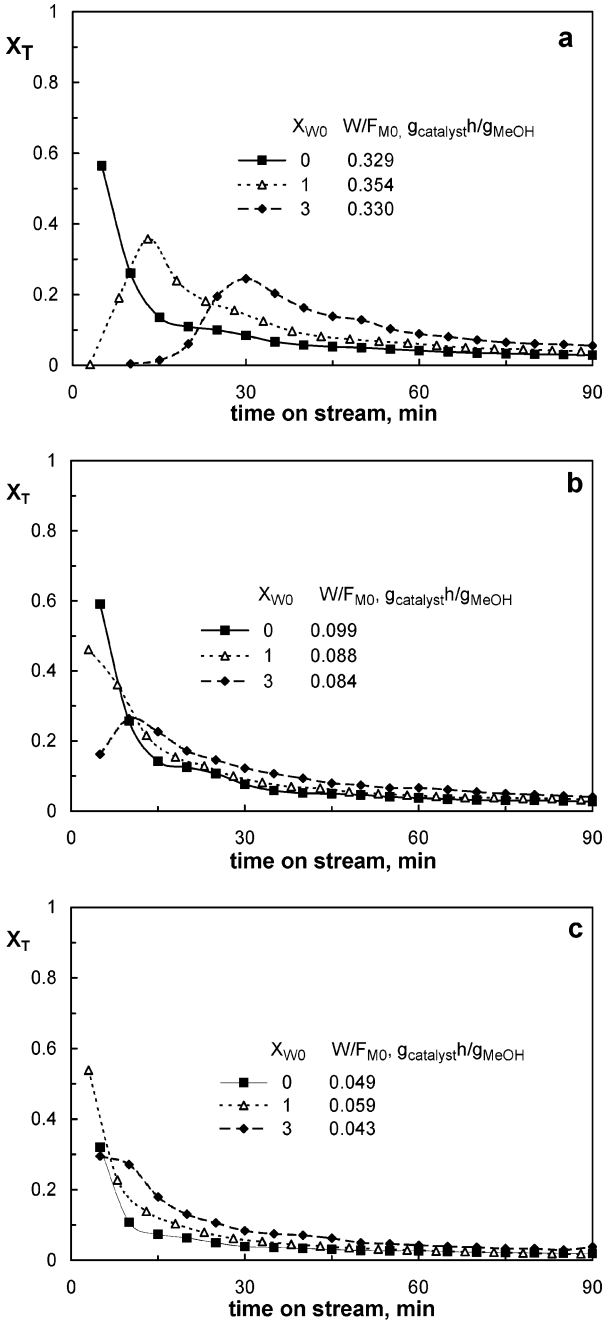

Figure 4. Evolution with time of the conversion to hydrocarbons for different water contents in the feed. (a) $T = 350$ °C and $W/F_{M0} \approx 0.33$ (g of catalyst)h(g of methanol)$^{-1}$. (b) $T = 400$ °C and $W/F_{M0} \approx 0.09$ (g of catalyst)h(g of methanol)$^{-1}$. (c) $T = 450$ °C and $W/F_{M0} \approx 0.05$ (g of catalyst)h(g of methanol)$^{-1}$.

the catalyst take part in the mechanism, which may be confused with the coke that deactivates the catalyst.[37]

The duration of the initiation period depends on the reaction conditions. Thus, in the runs carried out without diluting methanol with water in the feed (Figures 2a, 3a, and the results in Figure 4 corresponding to the feed without water), there is no initiation period. This period is clear in the remaining runs, in which water is fed with methanol.

In the graphs of Figure 4, it is observed that, for a given temperature, the maximum conversion is reached for higher values of time on stream as water content in the feed is higher. For a given water content in the feed ($X_{Wo} = 0$ in Figure 2a, $X_{Wo} = 1$ in Figure 2b, and $X_{Wo} = 3$ in Figure 2c), the duration of the initiation period and the time on stream corresponding to the maximum conversion considerably decrease as reaction temperature is increased, so that above 450 °C the maximum conversion is reached at almost zero time on stream.

Space time has no important influence on the duration of the initiation period (Figure 3), except for a very high water content in the medium (Figure 3c), and in this case, as space time is increased. the duration of this period decreases and the maximum conversion is reached for lower values of time on stream.

In view of these results, it is deduced that the variable of greater influence on the initiation period is water content in the reaction medium (water in the feed plus that produced in the reaction). In order to verify whether this effect is exclusively due to the presence of water and to its aforementioned inhibiting effect on the adsorption of methanol or whether it is due to the low

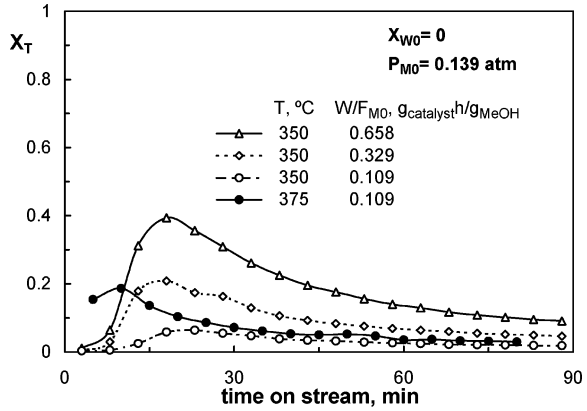

Figure 5. Evolution with time of the conversion to hydrocarbons for a feed of methanol diluted with nitrogen, at a low partial pressure of methanol. $Q_{N2} = 353$ cm^3 min^{-1}. $Q_T = 0.096$ cm^3 min^{-1}

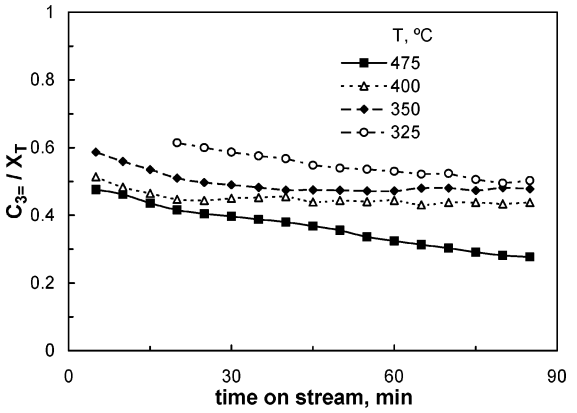

Figure 6. Effect of temperature on the selectivity to propene. $W/F_{M0} = 0.099$ (g of catalyst)h(g of methanol)$^{-1}$. $X_{W0} = 1$ (g of water)(g of methanol)$^{-1}$.

concentration of the reactant methanol, runs corresponding to Figure 5 have been carried out, in which there is no water in the feed, but methanol is diluted with N_2 to a partial pressure of 0.139 atm (that corresponding to a feed of methanol + water with 75 wt % water). It must be pointed out that the partial pressure of methanol in the runs without water in the feed is 0.795 atm, because a stream of N_2 is always fed in order to help the vaporization of methanol.

In Figure 5, an initiation period is observed in all the runs. The effect of the operating conditions on the position of the maximum conversion is similar to that aforementioned, and this position is not practically affected by space time but it is significantly affected by temperature. In fact, the maximum conversion is reached for lower values of time on stream as reaction temperature is increased.

When the effect of dilution with N_2 is compared to that corresponding to the dilution with water (75 wt % water, or $X_{W_o} = 3$), under the same partial pressure in the feed (0.139 atm), at the same temperature and space time, it is observed that the initiation period is longer when water is fed (~30 min) (Figure 3c) than when N_2 is fed (~20 min) (Figure 5). Consequently, apart from a mere feed dilution, water has an additional effect on the conversion, which consists of inhibiting the formation of active intermediate products in the production of olefins.

Effect of Operating Conditions on the Selectivity to Olefins. Figures 6 (for different temperatures), 7 (different space times), and 8 (different water contents

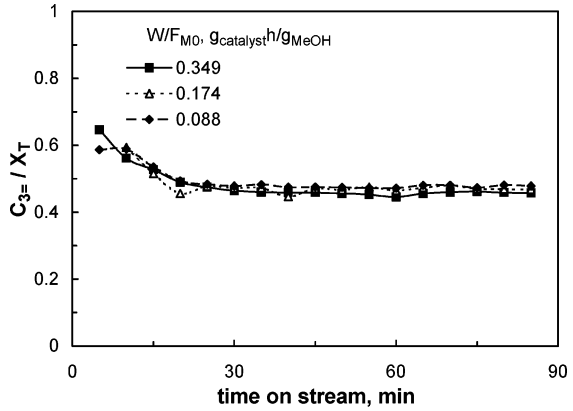

Figure 7. Effect of space time on the selectivity to propene. $T =$ 350 °C and $X_{W0} = 1$ (g of water)(g of methanol)$^{-1}$

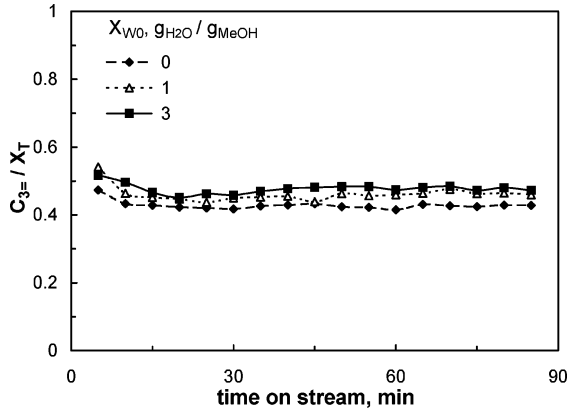

Figure 8. Effect of water content in the feed on the selectivity to propene at 400 °C and for $W/F_{M0} = 0.090$ (g of catalyst)h(g of methanol)$^{-1}$.

in the feed) show the results of evolution with time on stream of the selectivity to propene (main product under most operating conditions) for different operating conditions. Selectivity has been quantified as the ratio between the yield (in mass) of propene and the total conversion to hydrocarbons, X_T.

Figures 9−11 show the effect of each operating variable on the ratios between the yield of each olefin and the yield of propene.

The ethene/propene ratio is close (slightly lower) to 0.5 up to 400 °C and increases with temperature to values close to unity at 475 °C. Butenes/propene (Figure 9b) and pentenes/propene (Figure 9c) ratios peak at an intermediate temperature, ~400 °C, with values between 0.4 and 0.5 for the former and 0.12−0.15 for the latter. The decrease in the butenes/propene and pentenes/propene ratios at temperatures above 400 °C is a consequence of the fact that cracking reactions begin to be important above this temperature and therefore contribute to increasing the selectivity to light olefins (ethene and propene).

Space time has no significant effect on the selectivity to propene (Figure 7a) or to ethene (Figure 10a), although it is observed that as space time is increased there is a slight increase in the selectivity to butenes (Figure 10b) and to pentenes (Figure 10c).

The increase in the concentration of water in the reaction medium due to the increase of water in the feed causes a slight increase in the selectivity to propene (Figure 8). Given that ethene production is not significantly affected, the ethene/propene ratio decreases slightly as water content is increased (Figure 11a).

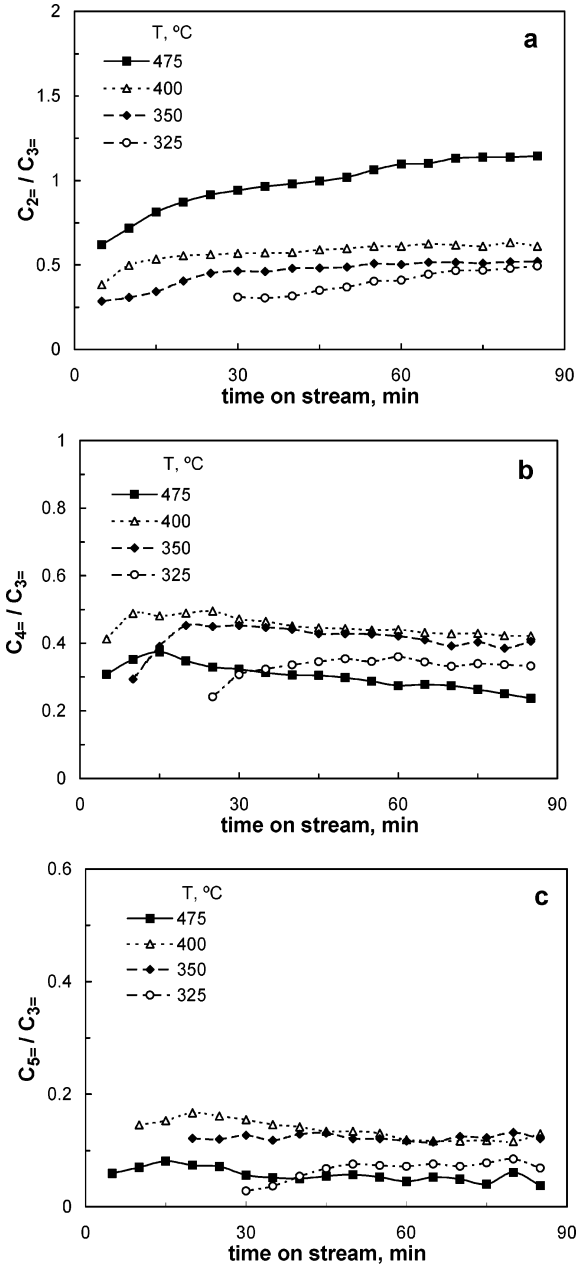

Figure 9. Effect of temperature on the ratios between the yield of each olefin and the yield of propene. W/F_{M0} = 0.099 (g of catalyst)h(g of methanol)$^{-1}$. X_{W0} = 1 (g of water)(g of methanol)$^{-1}$. (a) Ethene/propene. (b) Butenes/propene. (c) Pentenes/propene.

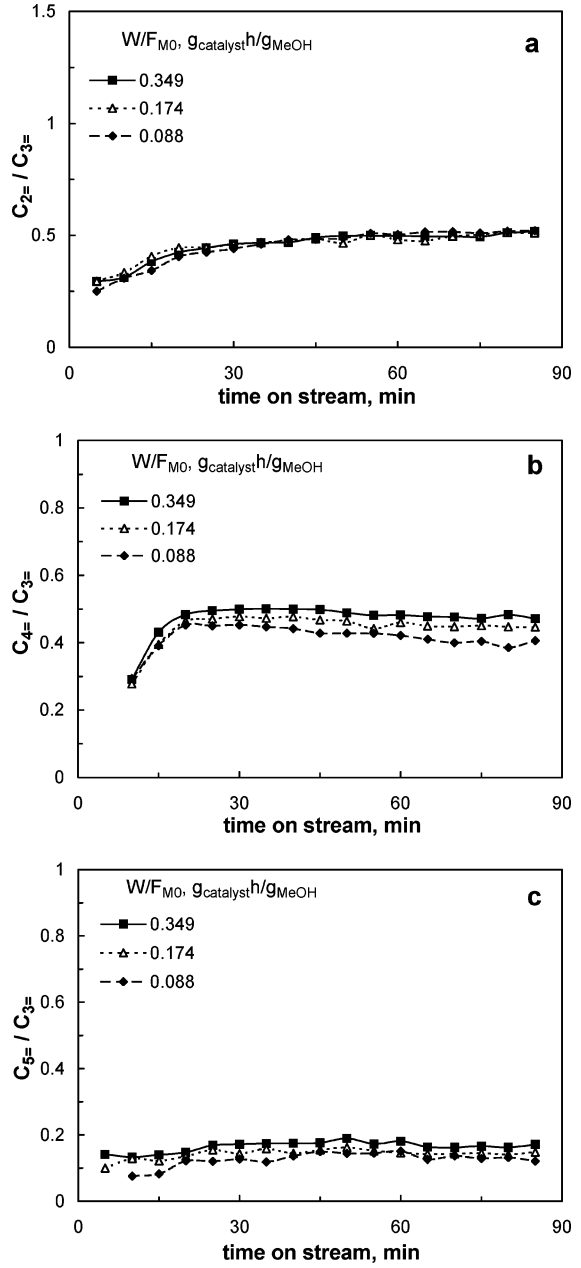

Figure 10. Effect of space time on the ratios of the yield of each olefin and the yield of propene. T = 350 °C and X_{W0} = 1 (g of water)(g of methanol)$^{-1}$. (a) Ethene/propene. (b) Butenes/propene. (c) Pentenes/propene.

Water in the feed slightly affects the production of butenes and pentenes, and consequently, butenes/propene (Figure 11b) and pentenes/propene (Figure 11c) ratios decrease as water content in the feed is increased.

The rapid deactivation by coke is noteworthy, and although it gives way to rapid pore blockage and a decrease in conversion (Figures 2−5), it does not have a significant effect on the evolution of selectivity to olefins. In Figures 9a, 10a, and 11a, it is observed that the ethene/propene ratio slightly increases with time on stream and this increase is less pronounced as deactivation is more severe. In some of the cases shown in Figures 9b, 10b, and 11b, the butenes/propene ratio also increases initially, but in these situations, the reaction is within the above-mentioned initiation period. After the initiation period, butenes/propene (Figures 9b, 10b, and 11b) and pentenes/propene (Figures 9c, 10c, and 11c) ratios are practically constant with time on stream.

Reactivity of Methanol and Dimethyl Ether. Figure 12 shows the results of evolution with time on stream of the ratio between the mass flow rate at the reactor outlet of methanol and dimethyl ether. The results correspond to 400 °C and each graph corresponds to a given water content in the feed. The horizontal dashed line indicates the value of the ratio for the thermodynamic equilibrium corresponding to the reaction conditions.

The results in Figure 12 show that, mainly in the initiation period (for low values of time on stream in Figure 12b and c), the methanol/dimethyl ether ratio is much higher than that corresponding to thermodynamic equilibrium. As the catalyst is being deactivated (affecting its capacity for producing olefins, but maintaining its capacity for dehydration of methanol to dimethyl ether), this ratio decreases and approaches that corresponding to equilibrium. The capacity for dehydration

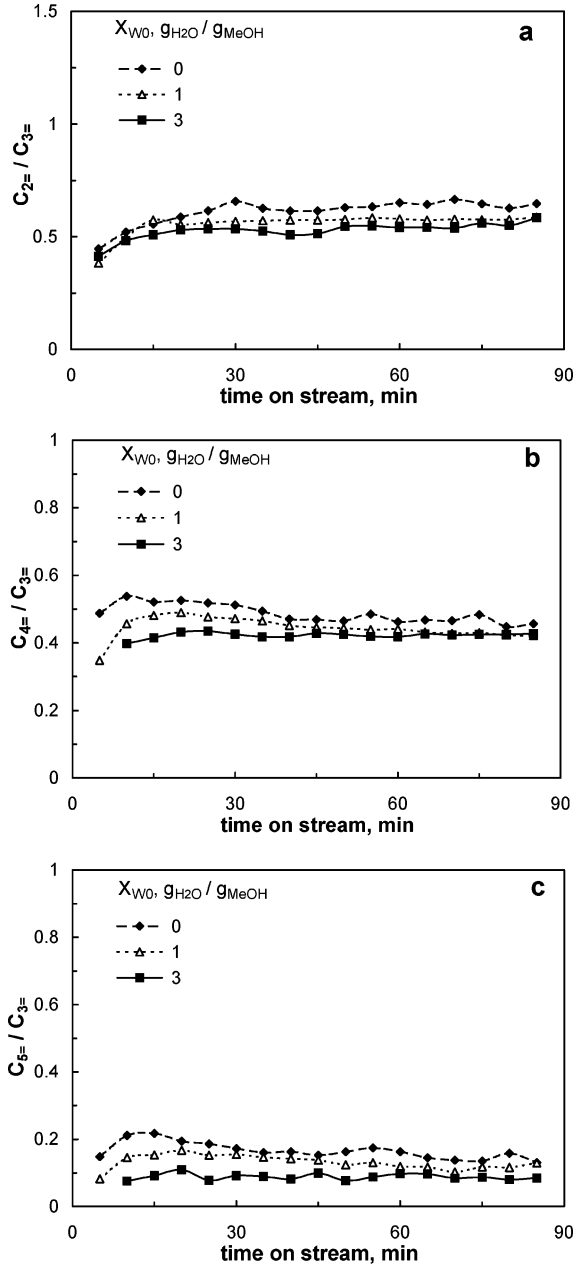

Figure 11. Effect of water content in the feed on the ratios between the yield of each olefin and the yield of propene at 400 °C and for $W/F_{M0} = 0.090$ (g of catalyst)h(g of methanol)$^{-1}$. (a) Ethene/propene. (b) Butenes/propene. (c) Pentenes/propene.

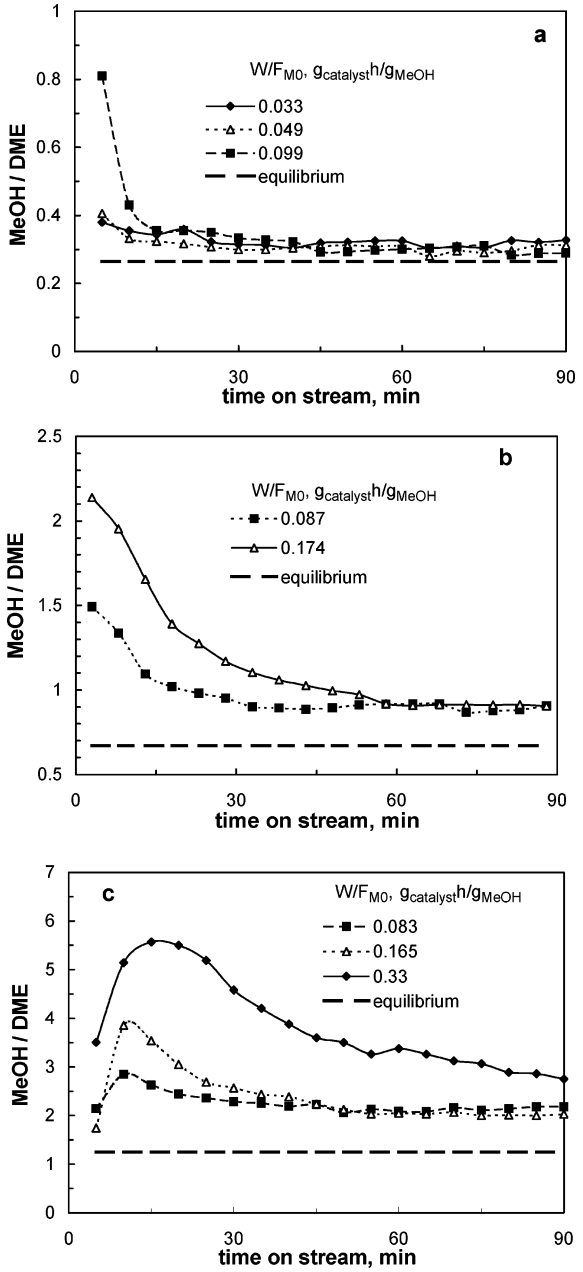

Figure 12. Evolution with time on stream of the ratio between the composition of methanol and dimethyl ether at the reactor outlet at 400 °C and for different values of space time. (a) $X_{Wo} = 0$ (g of water)(g of methanol)$^{-}$. (b) $X_{Wo} = 1$ (g of water)(g of methanol)$^{-}$. (c) $X_{Wo} = 3$ (g of water)(g of methanol)$^{-}$.

of methanol and a methanol/dimethyl ether ratio close to equilibrium are maintained under conditions in which the catalyst is considerably deactivated for olefin production.

These results are evidence that when SAPO-18 has residual activity (although this is small) for olefin production, dimethyl ether is more reactive than methanol. This higher reactivity of dimethyl ether has been observed in the transformation of methanol on HZSM-5 zeolite.[38,39]

Hydrothermal Stability of the Catalyst. Although the deactivation of SAPO-18 is slower than that of SAPO-34, activity and selectivity recovery is required for its use in the MTO process in operation by reaction−regeneration cycles, which in industry is carried out in a reactor−regenerator system where both units are fluidized beds with catalyst circulation.[40]

To check the hydrothermal stability of the catalyst, runs have been carried out in successive reaction−regeneration cycles. Regeneration has consisted in all cases of coke combustion with air at 550 °C for 2 h. This temperature has been selected because it is sufficiently high for ensuring total elimination of coke in a relatively short time but without exceeding the calcination temperature of the catalyst, to avoid deterioration of the acid structure during regeneration.[18] The reaction has been carried out at high temperatures (475 and 500 °C) and with a high water content in the reaction medium (50 and 75 wt % water in the feed), with the aim of checking the hydrothermal stability of the catalyst under the more severe reaction conditions. It must be pointed out that a temperature of 500 °C is already excessive for the MTO process because methane formation is significant. Figure 13 shows the results of

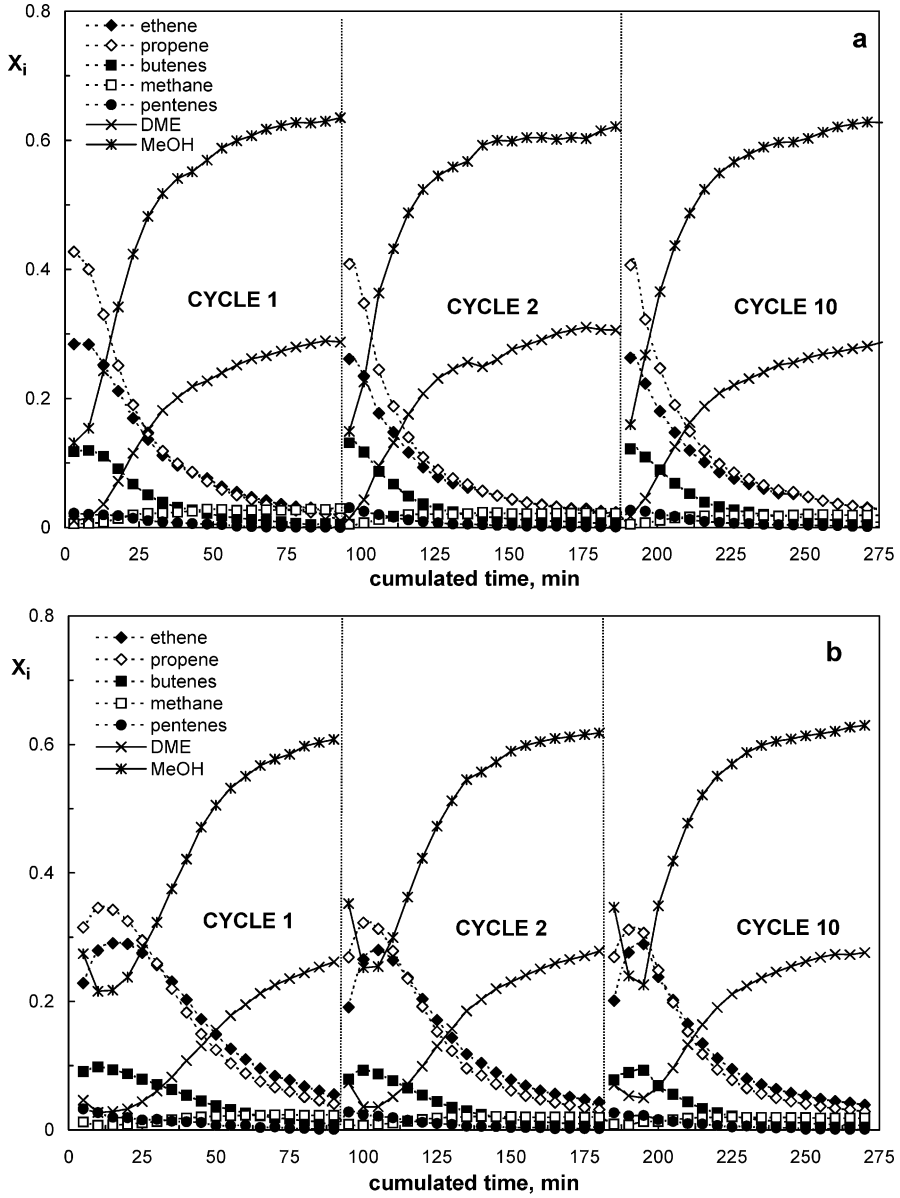

Figure 13. Evolution of the composition at the reactor outlet in reaction−regeneration cycles. (a) T = 475 °C, W/F_{Mo} = 0.177 (g of catalyst)h(g of methanol)$^{-1}$, X_{Wo} = 1 (g of water)(g of methanol)$^{-}$. (b) T = 500 °C, W/F_{Mo} = 0.33 (g of catalyst)h(g of methanol)$^{-1}$, X_{Wo} = 3 (g of water)(g of methanol)$^{-1}$.

evolution with time on stream of the mass fraction of the components at the reactor outlet for the fresh catalysts (first cycle), regenerated once (second cycle) and after nine reaction−regeneration cycles (tenth cycle). Each graph corresponds to different conditions in the reaction stage.

Reproducibility in the results of successive cycles is noteworthy, given that there is only a slight decrease in activity between the first and second reaction cycles, but after the second cycle the kinetic results are totally reproducible. This circumstance is unavoidable in acid catalysts, such as HZSM-5 zeolite,[41] which irreversibly lose some strongly acid Brönsted sites in the first regeneration, due to dehydroxylation and conversion to Lewis sites.

The high thermal stability of SAPO-18 under conditions of high temperature and high water content is similar to that of SAPO-34 and much higher than that shown for the catalyst based on HZSM-5 zeolite.[42−46] Buchholz et al.[47] studied thermal stability and dehydroxylation of Brönsted acid sites in several silicoaluminophosphates (HSAPO-18 included) after thermal treatments at 500−900 °C, by means of X-ray diffraction and multinuclear (^{1}H, ^{27}Al, ^{29}Si, ^{31}P) solid-state NMR spectroscopy. A dehydroxylation of at most 5% of the bridging OH groups (which are responsible for Brönsted acidity) was found after thermal treatments up to 600 °C, which indicates a high thermal stability of the Brönsted acid sites in these materials. After thermal treatment up to 900 °C, however, a dehydroxylation of 40−50% of the bridging OH groups occurred, but no change in the crystallinity of the SAPO framework takes place upon dehydroxylation. In contrast to the dehydroxylation of aluminosilicates, the dehydroxylation of silicoaluminophosphates was not accompanied by a dealumination of the framework, but rather by a removal of silicon (desilication) in the local structures of the bridging OH groups, which did not lead to the formation of defect OH groups. The high stability of the silicoaluminophosphates after dehydroxylation and desilication is explained by means of a healing process,

which is based on a migration of phosphorus atoms to framework vacancies and their transformation to $P(OAl)_4$ species.

Conclusions

It has been proven that SAPO-18 performs well in the MTO process, with a high selectivity for obtaining C_2-C_4 olefins and propene as the main product. The existence of an initiation period is noteworthy, and the duration of this period depends on the reaction conditions, particularly on water content in the feed and temperature. An increase in water content in the reaction medium contributes to increasing the duration of the initiation period and to attenuating the deactivation of the catalyst. An increase in temperature shortens the initiation period. It has been proven that the role of water in the reaction medium is, apart from that of diluent, that of an agent that inhibits the formation of active intermediates in the formation of olefins and, to a great extent, the evolution of these intermediates to coke. Consequently, water in the feed is a key condition to be optimized in the MTO process at industrial scale**.** This optimization requires kinetic models for the MTO process and for coke deactivation, in which the effect of water in the reaction medium must be taken into account.

The initiation period and its relationship with the operating conditions are evidence of the validity of the general hypotheses on the carbon pool mechanism, which will have to be taken into account in a future proposal of a kinetic model that quantifies the evolution with time on stream of the individual components of the MTO process. This model will have to take into account the existence of three consecutive periods: initiation, olefin production (which passes through a peak), and deactivation.

The variable of greater incidence on the selectivity to olefins is temperature, whose rise leads to an increase in the production of ethene and a decrease in the production of propene.

SAPO-18 is active for methanol dehydration to dimethyl ether even under conditions of low activity for olefin generation and with low values of space time. The higher concentration of methanol compared to the thermodynamic equilibrium in methanol dehydration is evidence of the higher reactivity of dimethyl ether over that of methanol in the mechanism of olefin formation.

SAPO-18 is of high hydrothermal stability, comparable to that already shown in the literature for SAPO-34. This feature is essential for the industrial application of SAPO-18 in the MTO process, where it is subjected to reaction−regeneration cycles.

Acknowledgment

This work was carried out with the financial support of the University of the Basque Country (Project 9/UPV 00069.310-13607/2001) and of the Ministry of Science and Technology of the Spanish Government (Project PPQ2003-5645).

Nomenclature

d_p = pore diameter, Å
P_{M0} = partial pressure of methanol in the feed, atm
T = temperature, °C
W/F_{M0} = space time, (g of catalyst)h(g of methanol)$^{-1}$
X_i = mass fraction of i component by mass unit of organic components in the product stream
X_T = total conversion to hydrocarbons
X_{W0} = water/methanol mass ratio in the feed

Literature Cited

(1) Waugh, K. C. Methanol Synthesis. *Catal. Today* **1992**, *15*, 51.

(2) Rostrup-Nielsen, J. R. Syngas in Perspective. *Catal. Today* **2002**, *712*, 243.

(3) Wu, J.; Saito, M.; Takeuchi, M.; Watanabe, T. The Stability of Cu/ZnO-Based Catalysts in Methanol Synthesis from a CO_2-rich Feed and from a CO-rich Feed. *Appl. Catal*. **2001**, *218*, 235.

(4) Chang, C. D.; Chu, C. T. W.; Socha, R. F. Methanol Conversion to Olefins over ZSM-5. I. Effect of Temperature and Zeolite Silica/Alumina Ratio. *J. Catal*. **1984**, *86*, 289.

(5) Gayubo, A. G.; Benito, P. L.; Aguayo, A. T.; Olazar, M.; Bilbao, J. Relationship Between Surface Acidity and Activity of Catalysts in the Transformation of Methanol into Hydrocarbons. *J. Chem. Technol. Biotechnol.* **1996**, *65*, 186.

(6) Kaeding, W. W.; Butter, S. A. Production of Chemicals from Methanol. I. Low-Molecular Weight Olefins. *J. Catal*. **1980**, *61*, 155.

(7) Chen, G.; Liang, J. Investigation of factors influencing selectivity and stability of catalysts for methanol conversion to lower olefins In *Proceedings of the China-Japan-U.S. Symposium on Heterogeneous Catalysis,* Dalian, China, 1982; paper A01C.

(8) Martin, A.; Nowak, S.; Lücke, B.; Wieker, W.; Fahlke, B. Coupled Conversion of Methanol and C_4−Hydrocarbons (CMHC) on Iron-Containing ZSM-5 Type Zeolites. *Appl. Catal.* **1990**, *57*, 203.

(9) Kikuchi, E.; Hatanaka, S.; Hamana, R.; Morita, Y. Acid Properties of ZSM-5 Type Zeolite and its Catalytic Activity in Methanol Conversion. *Int. Chem. Eng.* **1984**, *24*, 146.

(10) Howden, M. G. Zeolite ZSM-5 Containing Boron instead of Aluminium Atoms in the Framework. *Zeolites* **1985**, *5*, 334.

(11) Inui, T.; Medhanavyn, D.; Praserthdam, P.; Fukuda, K.; Ukawa, T.; Sakamoto, A.; Miyamoto, A. Methanol Conversion to Hydrocarbons on Novel Vanadosilicate Catalysts. *Appl. Catal*. **1985**, *18*, 311.

(12) Rodewald, P. G. Light Olefins. U.S. Patent 4,066,714, 1978.

(13) Yarlagadda, P.; Lund, C. R. F.; Ruckenstein, E. Conversion of Methanol to Hydrocarbons over Silica−Alumina: Selective Formation of Lower Olefins. *Appl. Catal.* **1989**, *54*, 139.

(14) Kaiser, S. W. Production of Light Olefins. U.S. Patent 4,-499,327, 1985.

(15) Kaiser, S. W. Methanol Conversion to Light Olefins over Silicoaluminophosphate Molecular Sieves. *Arabian J. Sci. Eng*. **1985**, *10*, 361.

(16) Marchi, A. J.; Froment, G. F. Catalytic Conversion of Methanol to Light Alkenes on SAPO Molecular Sieves. *Appl. Catal.* **1991**, *71*, 139.

(17) Aguayo, A. T.; Sánchez del Campo, A. E.; Gayubo, A. G.; Tarrío, A.; Bilbao, J. Deactivation by Coke of a Catalyst based on a SAPO-34 in the Transformation of Methanol into Olefins. *J. Chem. Technol. Biotechnol.* **1999**, *74*, 315.

(18) Aguayo, A. T.; Gayubo, A. G.; Atutxa, A.; Olazar, M.; Bilbao, J. Regeneration of a Catalyst Based on a SAPO-34 used in the Transformation of Methanol into Olefins. *J. Chem. Technol. Biotechnol.* **1999**, *74*, 1082.

(19) Wendelbo, R.; Akporiaye, D.; Anderson, A.; Dahl, I. M.; Mostad, H. B. Synthesis, Characterization and Testing of SAPO-18, MgAPO-18 and ZnAPO-18 in the MTO Reaction. *Appl. Catal.* **1996**, *142*, 197.

(20) Chen, J.; Wright, P. A.; Natarajan, S.; Thomas, J. M. Understanding the Bronsted Acidity of SAPO-5, SAPO-17, SAPO-18 and SAPO-34 and their Catalytic Performance for Methanol Conversion to Hydrocarbons. *Stud. Surf. Sci. Catal.* **1994**, *94*, 1731.

(21) Chen, J.; Thomas, J. M.; Wright, P. A.; Townsend, R. P. Silicoaluminophosphate Number Eighteen (SAPO-18): A new Microporous Solid Acid Catalyst. *Catal. Lett*. **1994**, *28*, 241.

(22) Vivanco, R. MTO Process (Methanol to Olefins). Alternative Catalysts and Kinetic Modelling for SAPO-18 Catalyst. Ph.D. Thesis, University of the Basque Country, Bilbao, Spain, 2004.

(23) Aguayo, A. T.; Gayubo, A. G.; Vivanco, R.; Olazar, M.; Bilbao, J. Role of Acidity and Microporous Structure in Alternative Catalysts for the Transformation of Methanol into Olefins. *Appl. Catal., A* **2005**, *283*, 197.

(24) Aguayo, A. T.; Gayubo, A. G.; Ortega, J. M.; Olazar, M.; Bilbao, J. Catalyst Deactivation by Coking in the MTG Process in Fixed and Fluidized Bed Reactors. *Catal. Today* **1997**, *37*, 239.

(25) Gayubo, A. G.; Aguayo, A. T.; Morán, A. L.; Olazar, M.; Bilbao, J. Role of Water in the Kinetic Modelling of Catalyst Deactivation in the MTG Process. *AIChE J.* **2002**, *48*, 1561.

(26) Gayubo, A. G.; Aguayo, A. T.; Sánchez del Campo, A. E.; Benito, P. L.; Bilbao, J. The Role of Water on the Attenuation of Coke Deactivation of a SAPO-34 Catalyst in the Transformation of Methanol into Olefins. *Stud. Surf. Sci. Catal.* **1999**, *126*, 129.

(27) Wu, X.; Anthony, R. G. Effect of Feed Composition on Methanol Conversion to Light Olefins over SAPO-34. *Appl. Catal., A* **2001**, *218*, 241.

(28) Alwahabi, S. M.; Froment, G. F. Single Event Kinetic Modeling of the Methanol-to-Olefins Process on SAPO-34. *Ind. Eng. Chem. Res.* **2004**, *43*, 5098.

(29) Kolboe, S. Methanol Reactions on ZSM-5 and other Zeolite Catalysts. Autocatalysis and Reaction-Mechanism. *Acta Chem. Scand. A-Phys. Inorg. Chem.* **1986**, *40*, 711.

(30) Dahl, I. M.; Kolboe, S. On the Reaction-Mechanism for Hydrocarbon Formation from Methanol over SAPO-34. 1. Isotopic Labeling Studies of the Co-Reaction of Ethylene and Methanol. *J. Catal.* **1994**, *149*, 458.

(31) Dahl, I. M.; Kolboe, S. On the Reaction-Mechanism for Hydrocarbon formation from Methanol over SAPO-34. 2. Isotopic Labeling Studies of the Co-Reaction of Propene and Methanol. *J. Catal.* **1996**, *161*, 304.

(32) Song, W.; Haw, J. F.; Nicholas, J. B.; Heneghan, C. S. Methylbenzenes Are the Organic Reaction Centers for Methanol-to-Olefins Catalysis on HSAPO-34. *J. Am. Chem. Soc.* **2000**, *122*, 10726.

(33) Haw, J. F.; Nicholas, J. B.; Song, W.; Deng, F.; Wang, Z.; Xu, T.; Heneghan, C. S. Roles for Cyclopentenyl Cations in the Synthesis of Hydrocarbons from Methanol on Zeolite Catalyst HZSM-5. *J. Am. Chem. Soc.* **2000**, *122*, 4763.

(34) Sassi, A.; Wildman, M. A.; Ahn, H. J.; Prasad, P.; Nicholas, N. B.; Haw, J. F. Methylbenzene Chemistry on Zeolite Hbeta: Multiple Insights into Methanol-to-Olefin Catalysis. *J. Phys. Chem. B* **2002**, *106*, 2293.

(35) Aguayo, A. T.; Gayubo, A. G.; Vivanco, R.; Alonso, A.; Bilbao, J. Initiation Step and Reactive Intermediates in the Transformation of Methanol into Olefins Over SAPO-18 Catalyst. *Ind. Eng. Chem. Res.*, in press.

(36) Chen, D.; Rebo, H. P.; Moljord, K.; Holmen, A. The Role of Coke Deposition in the Conversion of Methanol to Olefins over SAPO-34. *Stud. Surf. Sci. Catal.* **1997**, *111*, 159.

(37) Guisnet, M. Coke Molecules Trapped in the Micropores of Zeolites as Active Species in Hydrocarbon Transformations. *J. Mol. Catal. A: Chem.* **2002**, *182*, 367.

(38) Dewaele, O.; Geers, V. L.; Froment, G. F.; Marin, G. B. The Conversion of Methanol to Olefins: A Transient Kinetic Study. *Chem. Eng. Sci.* **1999**, *54*, 4385.

(39) Gayubo, A. G.; Aguayo, A. T.; Castilla, M.; Morán, A. L.; Bilbao, J. Role of Water in the Kinetic Modelling of Methanol Transformation into Hydrocarbons on HZSM-5 Zeolite. *Chem. Eng. Commun.* **2004**, *191*, 944.

(40) Keil, F. J. Methanol-to-Hydrocarbons: Process Technology. *Microporous Mesoporous Mater.* **1999**, *29*, 49.

(41) Benito, P. L.; Aguayo, A. T.; Gayubo, A. G.; Bilbao, J. Catalyst Equilibration for Transformation of Methanol into Hydrocarbons by Reaction−Regeneration Cycles. *Ind. Eng. Chem. Res.* **1996**, *35*, 2177.

(42) Liang, J.; Li, H.; Zhao, S.; Guo, W.; Wang, R.; Ying, M. Characteristics and Performance of SAPO-34 Catalyst for Methanol-to-Olefins Conversion. *Appl. Catal.* 1990, *64*, 31.

(43) Barger, P. T.; Lesch, D. A. Hydrothermal Stability of SAPO-34 in the Methanol-to-Olefins Process. *Arabian J. Sci. Eng.* **1996**, *21*, 263.

(44) Yarlagadda, P. S.; Yaoliang, H.; Bakhshi, N. N. Effect of Hydrothermal Treatment of HZSM-5 Catalyst on its Performance for the Conversion of Canola and Mustard Oils to Hydrocarbons, *Ind. Eng. Chem. Prod. Res. Dev.* **1986**, *25*, 251.

(45) de Lucas, A.; Cañizares, P.; Durán, A.; Carrero, A. Dealumination of HZSM-5 Zeolites: Effect of Steaming on Acidity and Aromatization Activity. *Appl. Catal.* **1997**, *154*, 221.

(46) Gayubo, A. G.; Aguayo, A. T.; Olazar, M.; Vivanco, R.; Bilbao, J. Kinetics of the Irreversible Deactivation of the HZSM-5 Catalyst in the MTO Process. *Chem. Eng. Sci.* **2003**, *58*, 5239.

(47) Buchholz, A.; Wang, W.; Xu, M.; Arnold, A.; Hunger, M. Thermal Stability and Dehydroxylation of Bronsted Acid Sites in Silicoaluminophosphates H-SAPO-11, H-SAPO-18, H.-SAPO-31 and H-SAPO-34 Investigated by Multi-Nuclear Solid-State NMR Spectroscopy. *Microporous Mesoporous Mater.* **2002**, *56*, 267.

Received for review January 27, 2005
Revised manuscript received May 17, 2005
Accepted June 8, 2005

IE050110K